Proof of a stable fixed point for strongly correlated electron matter

Jinchao Zhao, Gabriele La Nave, and Philip W. Phillips

Phys. Rev. B **108**, 165135 — Published 19 October 2023

DOI: 10.1103/PhysRevB.108.165135

Proof of a Stable Fixed Point for Strongly Correlated Electron Matter

Jinchao Zhao[1], Gabriele La Nave[2], and Philip W. Phillips[1]
[1]*Department of Physics and Institute for Condensed Matter Theory, University of Illinois 1110 W. Green Street, Urbana, IL 61801, U.S.A. and*
[2]*Department of Mathematics, University of Illinois, Urbana, Il. 61801*
(Dated: March 2023)

We establish the Hatsugai-Kohmoto model as a stable quartic fixed point (distinct from Wilson-Fisher) by computing the $\beta-$function in the presence of perturbing local interactions. In vicinity of the half-filled doped Mott state, the $\beta-$function vanishes for all local interactions regardless of their sign. The only flow away from the HK model is through the superconducting channel which lifts the spin degeneracy as does any ordering tendency. The superconducting instability is identical to that established previously [Phillips et al., Nature Physics, 16, 1175 (2020)]. A corollary of this work is that any system in which the spectral weight bifurcates into lower and upper bands such as the Hubbard model with repulsive interactions flows into the HK stable fixed point in the vicinity of half-filling. Consequently, although the HK model has all-to-all interactions, the bifurcation of the spectral weight is stable as nothing local destroys it. The consilience with Hubbard arises because both models break the Z_2 symmetry on a Fermi surface, the HK model being the simplest to do so. Indeed, the simplicity of the HK model belies its robustness and generality.

I. INTRODUCTION

Proving Mott's claim, in any dimension we care about ($d \geq 2$), that strong electron correlation opens a gap in a half-filled band without changing the size of the Brillouin zone still stands as a key unsolved problem in theoretical physics. Demonstrating that the spectral function contains no states in momentum space that cross the chemical potential would suffice as proof of Mott's claim. However, the inherent problem is that the model employed in this context, namely the Hubbard model, contains strong on-site repulsion in real space, thereby preventing any exact statement about the corresponding spectral function in momentum space. There is of course an easy way around this problem: add to the non-interacting band model an energy penalty, U,

$$H = \sum_{\mathbf{p}\sigma} \xi_{\mathbf{p}\sigma} n_{\mathbf{p}\sigma} + U \sum_{\mathbf{p}} n_{\mathbf{p}\uparrow} n_{\mathbf{p}\downarrow}, \tag{1}$$

whenever two electrons doubly occupy the same momentum state. The above $\xi_{\mathbf{p}\sigma}$ is the non-interacting band dispersion and $n_{\mathbf{p}\sigma}$ is the occupancy. Since such an interaction does not mix the momenta, a gap must open in the spectrum should U exceed the bandwidth as illustrated in Fig. 1. This is precisely the Hatsugai-Kohmoto model[1] which was introduced in 1992 but attracted essentially no attention until[2–12] our demonstration[13, 14] that this model offers an exact way of treating the Cooper instability in a doped Mott insulator. Despite this utility, the HK model faces an uphill battle to replace the ingrained Hubbard model as the knee-jerk response to the strong correlation problem with local-in-space interactions. In bridging the gap from the HK to the Hubbard model, three questions arise. 1) Does the HK model remain stable to local-in-space interactions? If it does, then a correspondence with the Hubbard model can be established. 2) Does the resilience to local-in-space interactions give rise to a stable fixed point? 3) What about the obvious spin degeneracy that arises from the singly occupied states in the spectrum? It is these three questions that we answer in this paper. Briefly, we construct the $\beta-$function explicitly and demonstrate that

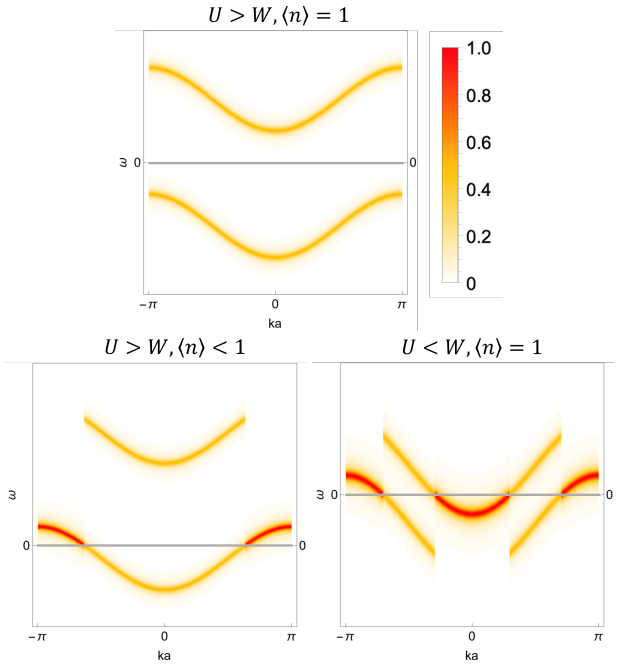

FIG. 1. The spectral functions of the HK model at different fillings and interaction strength. (**a**) Mott insulating state, with $U > W$ and $\langle n \rangle = 1$. (**b**) Strongly repulsive Mott metal, with $U > W$ and $\langle n \rangle < 1$. (**c**) Weakly repulsive Mott metal, with $U < W$ and $\langle n \rangle = 1$.

the answer to all three leading questions is yes. The degeneracy is lifted spontaneously by superconductivity as in a Fermi liquid which we demonstrate also obtains from an analogy of the Kohn-Luttinger effect[15]. Independently, recent work by Manning-Coe and Bradlyn[16] shows that the zeroes of the HK model survive even if the degeneracy is lifted in the Mott insulating state through a 2-orbital generalization of the HK or effectively a transition to the orbital HK model. Further, the zeroes that persist are sufficient to describe a Mott insulator even when the spin-rotation symmetry is broken[16] (see

Fig. 4 of Manning-Coe/Bradlyn). This once again connects with our previous K-theory argument[14] that as long as the Luttinger surface of zeros exists, the mechanism used to create it is irrelevant. It is simply connected and stable to all local perturbations such as the operators used to describe antiferromagnetism/pseudogap order. This is supported experimentally. Namely, the spectral weight transfer observed in the cuprates[17] persists even above any temperature having to do with antiferromagnetic order. That is, Mottness is independent of the spin state that ensues at low temperatures.

As Fermi liquids admit a purely local description in momentum space, their eigenstates are indexed simply by momentum and spin. Consequently, in real space, Fermi liquids exhibit long-range entanglement. It is precisely this long-range entanglement that makes them impervious to any local interaction, that is, short-range Coulomb interactions. The renormalization group analysis of a Fermi liquid shows distinctly[18, 19] that should the sign of the interaction be reversed and the electrons reside on opposites of the Fermi surface, a superconducting instability arises. The added stipulation of the electrons residing on opposite sides of the Fermi surface changes the scaling dimension of the generic 4-fermion interaction from being irrelevant to marginal. Also of note is that in terms of the pair annihilation operator, $b_k = c_{k\uparrow}c_{k\downarrow}$, the Cooper pairing interaction

$$V_{\rm pair} = -g\sum_{\mathbf{k},\mathbf{k}'} b^\dagger_{\mathbf{k}} b_{\mathbf{k}'}, \tag{2}$$

is completely non-local in real space as it involves an interaction between all pairs of electrons regardless of their separation. Such non-locality does not make the BCS model unphysical because this interaction is the only relevant perturbation that destroys a Fermi liquid as indicated by the 1-loop flow equation,

$$\frac{dg}{dt} = \frac{g^2}{4\pi}, \tag{3}$$

which exhibits a breakdown at a finite energy scale (the transition temperature) signaling the onset of pairing and the eventual non-perturbative physics of the BCS superconducting state. All of this is summarized in the flow diagram in Fig. (2): short-range interactions ($V_{\rm local}$) regardless of their sign flow to the Fermi liquid state while the Cooper term, ($V_{\rm pair}$), inherently non-local in real space, flows to strong coupling. Once again, it is the real-space long-range entanglement of a Fermi liquid that accounts for its resilience to any short-range interaction.

As it is ultimately the conservation of the charge currents in momentum space, $n_{\mathbf{p}\sigma}$, that is at play here, it is natural to rewrite the HK model as $\sum_p h_p$ with h_p implicitly defined from Eq. (1). From this, it is clear that the HK model has a momentum-diagonal structure of a Fermi liquid. However, unlike a Fermi liquid, this model describes a Mott insulator[1, 13, 14] as shown in Fig. (1). While it is natural to criticize this model as being unphysical because of the non-local in real space interactions, non-locality by itself does not dismiss

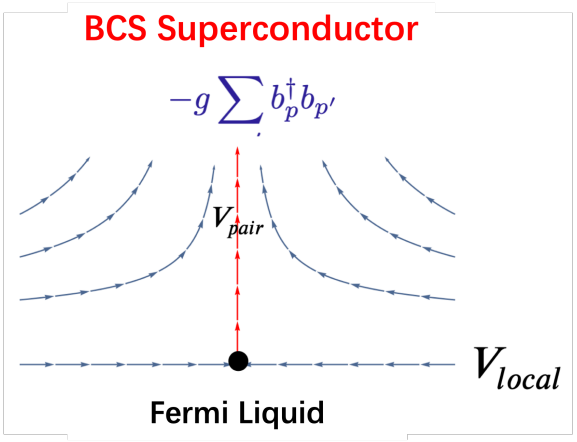

FIG. 2. Perturbative low diagram for interactions in a Fermi liquid. Short-range interactions regardless of their sign do nothing. Pairing leads to a flow to strong coupling and the ultimate destruction of the Fermi liquid and the onset of a superconducting state. The nature of the superconducting state cannot be established based on perturbative arguments but requires BCS theory.

a model from being physically relevant as $V_{\rm pair}$ in a Fermi liquid is non-local but nonetheless is the only relevant pairing term that leads to the BCS instability. The real question is: Do local interactions lead to flow away from the Hatsugai-Kohmoto model? That is, does the doped Mott insulator that HK describes represent a fixed point in direct analogy with the stability of a Fermi liquid to local interactions? We show here that the answer to this question is a resounding yes; HK is a stable fixed point. Even adding local terms of the Hubbard kind does nothing.

Analogies with Fermi liquid aside, a more fundamental reason is operative for the resilience of the HK model to local perturbations. Haldane and Anderson[20] argued that Fermi liquids contain an added Z_2 symmetry on the Fermi surface that amounts to a particle-hole interchange for one of the spin species. Operationally, if only doubly occupied or empty sectors are present, adding or removing an electron of either spin is kinematically equivalent. However, removing an electron from a singly occupied k-state can only be done in one way, thereby breaking the Z_2 symmetry. Note even in the Hubbard model, the on-site repulsion creates single occupancy in real space which will give rise to single occupancy also in momentum space. HK suffices as it is the simplest term that does so[14]. As long as this symmetry is already broken, adding new interactions that also break this symmetry yields no relevant physics as far as Wilsonian renormalization is concerned.

We carry out the full renormalization group analysis for the HK model and show that as in a Fermi liquid, no local perturbation destroys the HK model, thereby defining a stable fixed point. The only perturbation that destroys HK physics is $V_{\rm pair}$ as in a Fermi liquid. We conclude then that the HK model is more than a toy model. Rather it represents a stable fixed point for a model non-Fermi liquid that describes a Mott insulator. It is a new fixed point in quantum matter that describes a doped Mott insulator. The superconducting state that ensues[13] is

the BCS analogue for a doped Mott insulator.

II. RUMINATION ON LANDAU'S FERMI LIQUID THEORY

Before we begin the RG for the HK model, we take a closer look at Landau's formulation of the Fermi liquid theory. At the heart of his articulation of this theory is the energy functional for the momentum near the Fermi surface,

$$E[\delta n_{k\sigma}] = \sum_k (\epsilon(k) - \epsilon_F) n_{k\sigma} + \frac{1}{2}\sum_{k,k'} f_{k\sigma,k'\sigma'} \delta n_{k\sigma} \delta n_{k'\sigma'}, \tag{4}$$

where $f_{k\sigma,k'\sigma'}$ are the Landau parameters. These Landau parameters are then the zero-momentum limit of the local in real space interactions,

$$H_f = \sum_{p,p',\sigma\sigma',|q|<\Lambda} f_{p\sigma,p'\sigma'}(q) n_{p\sigma}(q) n_{p'\sigma'}(q), \tag{5}$$

and $f_{p\sigma,p'\sigma'} = f_{p\sigma,p'\sigma'}(q \to 0)$. Although Landau did not have RG at his disposal, his intuition that the interactions do not destroy the quasiparticle picture stands. What RG[18, 19] has taught us is that the Landau Fermi liquid is described by the forward scattering Landau parameters in H_f (zero-angle or small-angle scattering), which are the only marginal interactions in the absence of the BCS instability. There is an important caveat that is relevant to the HK model. Namely, forward scatterings in FL theory must correspond entirely to local-in-space interactions. Consequently, completely absent from any applicability of Landau's FL theory is the term in which $k = k'$, that is, $f_{k\sigma,k'\sigma} = U\delta_{k,k'}\delta_{\bar{\sigma},\sigma'}$. That this term lies outside Landau's FL theory is seen simply by power counting. Because of the single momentum integration, this term has scaling dimension -2 and hence is a relevant perturbation to FL theory.

Why should anyone consider a non-local HK interaction? The answer is simple. If RG tells us it is a relevant interaction, then it behooves us to take it seriously. After all, relevant interactions define fixed points and hence tell us about universal physics. As in Landau's formulation, HK's work did not rely on the RG principle. It was presented simply as a model that leads to a bifurcation of the spectral weight per momentum state and hence a Mott insulating state should $U > W$. In our previous work[14], we pointed out that the HK interaction is important because it is the simplest that breaks the Z_2 symmetry of a Fermi liquid. The half-filling Mott insulating state driven by HK holds the Luttinger surface as a fixed point. Here we take this observation further and show that the metallic state that ensues cannot be described by FL theory because the relevant scaling of $Un_{k\uparrow}n_{k\downarrow}$ leads to the flow away from the FL fixed point. Given how problematic progress has been on the Mott problem, numerical simulation is the primary tool, if the key features of this problem can be obtained by analyzing a quartic fixed point, this is reason enough to take the HK model seriously. Indeed while locality has its place, the solvability of models which break the Z_2 symmetry of a Fermi surface makes the exploration of a possible fixed point that governs this physics paramount. With this fixed point, all interactions that might be thought to be relevant to Mott physics can be analyzed within the lens of relevance in the RG sense. What we show here is that none leads to flow away from the HK fixed point except for superconductivity. Our conclusion then is that long-range interactions are instrumental in producing the Hubbard bands. This is not surprising given that hopping among all the lattice produces the non-interacting band structure. For strong correlations, short-range correlations should drive local-moment formation while it is the effective long-range part of the interaction that produces anything like a band in momentum.

What about antiferromagnetism (AF) which is clearly absent from the HK model? As AF emanates from the Mott state, it is subservient to it. That is, it is a detail of Mott physics not a defining feature of it. That is, it cannot change the existence of the HK Mott fixed point. What we consider here is the metallic (or doped) state arising from this model. What is relevant to show here is that the bifurcation of the spectral weight into lower and upper Hubbard bands, thereby breaking the 1-1 correspondence of Landau leads to a new metallic quartic fixed point.

III. RG APPROACH FOR $d \geq 2$ HK MODEL: TREE LEVEL ANALYSIS

Our goal is to establish the stability of the HK model to weak local interactions. Central to the HK model are the two filling surfaces, the lower filling surface (L-surface) separates singly-occupied and empty states, and the upper filling surface (U-surface) separates the doubly- and singly- occupancy. The key argument of the RG process is that at weak coupling, only modes around these filling surfaces participate. At different filling and interaction strengths, the number of filling surfaces varies from zero (Mott insulating state, Fig.1(a)), to one (strongly repulsive Mott metal, Fig.1(b)) or two (weakly repulsive Mott metal, Fig.1(c)). For simplicity, we work with $d = 2$ and rotationally invariant filling surfaces. The higher dimensional result can always be achieved by adding rotational degrees of freedom and the relevance of interactions that define the fixed point is not changed.

The phase space argument for the quasiparticle decay in a Fermi liquid can be recast here for the HK model. The propagating mode of the HK model separates into two components $c_{K\sigma} = \psi^1_{K\sigma} + \psi^2_{K\sigma}$, where the holon $\psi^L_{K\sigma} = c_{K\sigma}(1 - n_{K\bar{\sigma}})$ with energy $E^L_K = \xi_K$ and the doublon $\psi^U_{K\sigma} = c_{K\sigma} n_{K\bar{\sigma}}$ with energy $E^U_K = \xi_K + U$. Every fermion operator that participates in the interacting process can be split into these two components. The decaying process that involves a quasiparticle 1 decaying into a quasiparticle 2 and a particlehole pair 3, 4 includes energy conservation: $\Gamma(\varepsilon = E_1^{\alpha_1}) \propto \delta(\varepsilon - E_2^{\alpha_2} - E_3^{\alpha_3} + E_4^{\alpha_4})$, where $\alpha_1, \alpha_2, \alpha_3, \alpha_4 = L/U$ represents the holon/doublon index for each momentum participating in the scattering process. For a large enough U, the number of holon/doublon has to be conserved so as to achieve the energy conservation implied by the delta function. Ac-

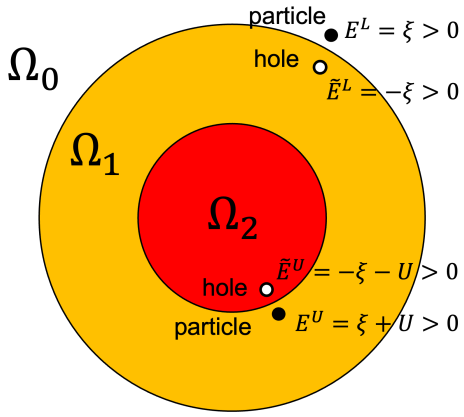

FIG. 3. The filling surfaces of the HK model as defined by the boundary between region Ω_0 (empty), Ω_1 (singly-occupied), and Ω_2 (doubly-occupied). Adding a particle to the ground state in Ω_0 costs a positive energy $E^L = \xi > 0$, adding a particle in Ω_1 costs a positive energy $E^U = \xi + U > 0$, and adding a particle in Ω_2 is prohibited by Pauli principle. Removing a particle from the ground state, equivalent to adding a hole in Ω_0, is prohibited, adding a hole in Ω_1 costs a positive energy $-E^L = -\xi > 0$, and adding a hole in Ω_2 costs a positive energy $-E^U = -\xi - U > 0$.

cording to Figure 3, we further recognize that in the ground state, the outgoing quasiparticles E_2 and E_3 are always positive regardless of whether they represent the holon or doublon excitations. The outgoing quasihole $\tilde{E}_4 = -E_4$, on the other hand, is also positive regardless of whether it represents holon or doublon removal. Thus, the phase space for the decaying scattering for a general interaction is suppressed by the same factor ε^2 as in Fermi liquid, guaranteeing the validity of the low energy cutoff description that sets up the RG.

A. L-surface

We start with the analysis of the setup with only one spherical filling surface of which the particle occupancy is singly- or empty on either side (L-surface). This analysis follows the method by Weinberg[21] and Shankar[19] though we use the notation of Polchinski[18]. The L-surface is defined by $\xi_{\mathbf{K}_L} = 0$, and we linearize the dispersion around the L-surface with radius K_L to

$$\xi_{\mathbf{K}=\mathbf{n}(K_L+k)} = v_L k, \tag{6}$$

where $\mathbf{n} = \frac{\mathbf{K}}{|\mathbf{K}|}$ is the unit vector in the direction of $\mathbf{K}$ and v_L is the isotropic L-surface velocity. Note linearization restricts our analysis to the vicinity of the metallic state where Mott physics is relevant. Near the bottom of the band, our analysis fails as the band dispersion is inherently quadratic, and weak coupling physics is obtained. We write the zero temperature partition function,

$$Z = \int \mathcal{D}[c,\bar{c}]e^{-S_0}, \tag{7}$$

$$S_0 = \int_\Lambda \frac{d^d\mathbf{K}}{(2\pi)^d}\int_{-\infty}^{\infty} d\omega \left[\sum_\sigma \bar{c}_{\mathbf{K}\sigma}(i\omega - v_L k)c_{\mathbf{K}\sigma} + U\bar{c}_{\mathbf{K}\uparrow}\bar{c}_{\mathbf{K}\downarrow}c_{\mathbf{K}\downarrow}c_{\mathbf{K}\uparrow}\right]. \tag{8}$$

The integral over momentum is confined in a thin shell around the filling surface, with distance Λ as the cut-off. The partition function factorizes at each momentum K, in exactly the same ways as a Fermi liquid, however, mixing the up and down spins at the same momentum. After integrating out the fast modes living within $s\Lambda < |k| < \Lambda$, we perform the rescaling of the variables and fields:

$$k' = s^{-1}k, \tag{9}$$

$$\omega' = s^{-1}\omega, \tag{10}$$

$$c'_{\mathbf{K}'\sigma} = s^{3/2}c_{\mathbf{K}\sigma}, \tag{11}$$

$$U' = s^{-2}U, \tag{12}$$

to make the partition function invariant up to a constant. It is worth noting that the HK repulsion has a scaling dimension of -2 and hence is strongly relevant. This relevant term suppresses the contribution of spectral weight from the other band that is U away from the filling surface.

Now we consider the effect of perturbations on this fixed point. First, consider perturbations that are quadratic in the fields,

$$\delta S^{(2)} = \int_\Lambda \frac{d^d\mathbf{K}}{(2\pi)^d}\int_{-\infty}^{\infty} d\omega \sum_\sigma \mu(\mathbf{K})\bar{c}_{\mathbf{K}\sigma}c_{\mathbf{K}\sigma}. \tag{13}$$

This action separates into slow and fast pieces, and the effect of integrating out the fast modes produces a constant. After rescaling the momenta and the fields, we have

$$\mu'(k') = s^{-1}\mu(k). \tag{14}$$

This relevant term is the chemical potential, which should be included in the action kinetic term. As a result, the location of the fixed point definitely depends on the filling of the system. We shall adjust the position of the filling surface according to the chemical potential so as to make the system truly fixed.

Next, we consider the quartic interaction in the most general form,

$$\begin{aligned}
\delta S_4 &= \int_K\int_\omega \bar{c}_4(\omega_4)\bar{c}_3(\omega_3)c_2(\omega_2)c_1(\omega_1)u(4,3,2,1),\\
\bar{c}_i &\equiv \bar{c}_{\mathbf{K}_i\sigma_i},\\
c_i &\equiv c_{\mathbf{K}_i\sigma_i},\\
u(4,3,2,1) &= u(\mathbf{K}_4\sigma_4,\mathbf{K}_3\sigma_3,\mathbf{K}_2\sigma_2,\mathbf{K}_1\sigma_1),\\
\int_K &\equiv \prod_{i=1}^4\int_\Lambda d\mathbf{K}_i\int d\Omega_i\delta(\mathbf{K}_1+\mathbf{K}_2-\mathbf{K}_3-\mathbf{K}_4),\\
\int_\omega &\equiv \prod_{i=1}^4\int_{-\infty}^{\infty} d\omega_i\delta(\omega_1+\omega_2-\omega_3-\omega_4).
\end{aligned} \tag{15}$$

The delta functions put constraints on the integral region of momentum and frequency. The delta function on frequency could be easily rescaled as $\delta(\omega_1' + \omega_2' - \omega_3' - \omega_4') = s\delta(\omega_1 + \omega_2 - \omega_3 - \omega_4)$ since the integral over frequency extends to infinity. The delta function on momentum, however, has a different scaling behavior as pointed out by Polchinski[18]. The distance from the filling surface only gives a contribution proportional to the cutoff Λ which is a negligible contribution compared with the filling momentum K_L : $\delta(\mathbf{K}_1 + \mathbf{K}_2 - \mathbf{K}_3 - \mathbf{K}_4) \approx \delta(K_L(\mathbf{n}_1 + \mathbf{n}_2 - \mathbf{n}_3 - \mathbf{n}_4) + O(\Lambda))$. When the momenta all point in different directions, the first term in the delta function dominates and the delta function does not scale upon RG. Following the same argument by Polchinski[18], this quartic operator is thus irrelevant at the tree level,

$$u'(4', 3', 2', 1') = su(4, 3, 2, 1). \tag{16}$$

It is then easy to see that any further interactions are even more irrelevant. This power-counting tree-level analysis already rules out the general short-range interactions from being relevant. Upon decreasing the energy scale, we find that the coupling becomes weaker and weaker while the HK repulsion gets stronger and stronger. Consequently, Mott physics captured by the filling surface is stable under local interactions.

There is an important subtlety in the kinematics and as a result, our treatment of the delta function is not always valid. The first-term contribution to the delta function could be set exactly to zero by putting an additional constraint on the momentum directions. The second term which is proportional to Λ will be renormalized and generates a factor of s. The rescaling of these direction-constrained interactions are

$$u'(4', 3', 2', 1') = s^0 u(4, 3, 2, 1). \tag{17}$$

Performing a Taylor expansion in k and ω and comparing coefficients of separate powers, we conclude that the leading term, with no dependence on either variable, is marginal, while all the rest are irrelevant. Because there are only two degrees of freedom in momentum, both of them are non-local by definition. Consequently, to reach a definitive conclusion, we must proceed to the 1-loop level to determine whether they are marginally irrelevant or marginally relevant, or truly marginal. This calculation will be performed in the next section.

B. U-surface

In the case that the filling surface is the occupancy boundary of the doubly and singly occupied regions, the U-surface is defined by $\xi_{\mathbf{K}_U} + U = 0$. We have to perform an extra particle-hole transform before we write down the partition function in the path integral language so as to obtain the correct linearized dispersion around the U-surface with radius K_U,

$$\xi_{\mathbf{K}=\mathbf{n}(K_U+k)} + U = v_U k. \tag{18}$$

This particle-hole asymmetry reflects the broken Z_2 symmetry of Mott physics. The zero temperature partition function then becomes

$$Z = \int \mathcal{D}[c, \bar{c}] e^{-S_0}, \tag{19}$$

$$S_0 = \int_\Lambda \frac{d^d\mathbf{K}}{(2\pi)^d} \int_{-\infty}^{\infty} d\omega \left[\sum_\sigma \bar{c}_{\mathbf{K}\sigma}(i\omega - v_U k) c_{\mathbf{K}\sigma} + U \bar{c}_{\mathbf{K}\uparrow} \bar{c}_{\mathbf{K}\downarrow} c_{\mathbf{K}\downarrow} c_{\mathbf{K}\uparrow} \right]. \tag{20}$$

Choosing the same setup with cut-off Λ results in the same scaling rule for the variables and fields as in Eq.(12). The identical analysis on quadratic and quartic perturbations thus reoccurs and we have the same irrelevant tree-level behavior around this U-surface fixed point.

C. 2 Filling Surfaces

In the weakly repulsive case, the 2 occupancy boundaries (L-surface and U-surface) coexist. In order to discuss low-energy physics, we have to include modes around both filling surfaces. Due to the factorizability of the partition function in momentum space, we can safely achieve the bare partition function by the product of Eq.(7) and Eq.(19). By setting the energy scale Λ around both filling surfaces to be the same, we arrive at the same scaling of the variables and fields as in Eq.(12). In conclusion, regardless of the number of filling surfaces, local interactions are always irrelevant at the tree level and hence do not modify the fixed point defined by the filling surfaces. We will move on to see the effect of marginal quartic interactions on these fixed points.

IV. THE PERTURBATIVE EXPANSION FOR 1-LOOP LEVEL CORRECTIONS

With the tree-level analysis in hand, we have already ruled out the local part of any perturbations. It is interesting to see how we can obtain a collective effect such as superconductivity in a low-energy theory.

The RG process is carried out by integrating the fast modes and rescaling the slow modes and the associated variables to keep the partition function unchanged. Besides the terms that only contain slow modes(tree-level result), we also need to include the terms that have both slow modes and fast modes and add their contribution to the scaling equations. This process is mathematically equivalent to calculating multipoint correlation functions with interactions. In the HK model, the correlation functions could be calculated using perturbative expansion for weak coupling as demonstrated in the Appendix.

The increment in $u(4, 3, 2, 1)$

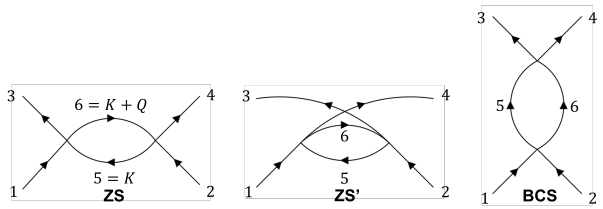

FIG. 4. The one-loop graphs for $\beta(u)$ for quartic interactions. The loop momenta lie in the shell of width $d\Lambda$ being eliminated. The external frequencies being all zero, the loop frequencies are (a) equal for ZS, (b) equal for ZS', and (c) opposite for the BCS graph.

$$\begin{aligned} du(4,3,2,1) = &\int u(6,3,5,1)u(4,5,2,6)G(5)G(6)\delta(3+6-1-5)d5d6 \\ &- \int u(6,4,5,1)u(3,5,2,6)G(5)G(6)\delta(6+4-1-5)d5d6 \\ &- \frac{1}{2}\int u(6,5,2,1)u(4,3,6,5)G(5)G(6)\delta(5+6-1-2)d5d6. \end{aligned} \tag{21}$$

is given by 3 diagrams as mentioned by Shankar[19], and we will follow the nomenclature to call them ZS, ZS' and BCS diagrams respectively.

We examine first the tree-level marginal interactions. We define the momentum components on the filling surface of K_i as K_i^F. Then a common property of these marginal interactions is that the sum of the incoming and outgoing K_i^Fs is zero $\mathbf{K}_1^F + \mathbf{K}_2^F - \mathbf{K}_3^F - \mathbf{K}_4^F = 0$. The delta function on momentum thus scales as s^{-1} and gives the marginal power counting. This property reduces the marginal interactions into two families: 1) forward scatterings and 2) superconducting pairings or the Cooper channel.

V. FORWARD SCATTERINGS AT 1-LOOP

The forward scatterings are defined by a non-vanishing $\mathbf{P} = \mathbf{K}_1^F + \mathbf{K}_2^F$. This nomenclature comes from the $d = 2$ 1-filling surface case, where there are only two solutions: $\mathbf{K}_1 = \mathbf{K}_3, \mathbf{K}_2 = \mathbf{K}_4$ or $\mathbf{K}_1 = \mathbf{K}_4, \mathbf{K}_2 = \mathbf{K}_3$. These two setups are equivalent to one another up to changing the Fermion order.

A. 1 Filling surface

When there is only a single filling surface, the forward scattering is determined only by the solution to $\mathbf{K}_1 = \mathbf{K}_3, \mathbf{K}_2 = \mathbf{K}_4$. Including spins, there are explicitly 3 choices:

$$F^1(\mathbf{n}_1, \mathbf{n}_2) = u(\mathbf{K}_2\sigma, \mathbf{K}_1\sigma, \mathbf{K}_2\sigma, \mathbf{K}_1\sigma), \tag{22}$$

$$F^2(\mathbf{n}_1, \mathbf{n}_2) = u(\mathbf{K}_2\bar{\sigma}, \mathbf{K}_1\sigma, \mathbf{K}_2\bar{\sigma}, \mathbf{K}_1\sigma), \tag{23}$$

$$F^3(\mathbf{n}_1, \mathbf{n}_2) = u(\mathbf{K}_2\sigma, \mathbf{K}_1\bar{\sigma}, \mathbf{K}_2\bar{\sigma}, \mathbf{K}_1\sigma). \tag{24}$$

Due to the fact that any higher order terms in the Taylor expansion on ω and k are irrelevant, we can freely choose the frequency and momentum deviations. For simplicity, we set all external legs to zero frequency and almost on the filling surface ($\omega = 0, k = \epsilon \ll d\Lambda$). The tiny value of ϵ will be set equal to zero at the last step. We need to keep it during the calculation to make the running momentum K and $K+Q$ distinct according to the requirement of the weak coupling expansion (See Appendix).

First, we consider the ZS diagram in Fig.4 given by the first integral in Eq.(21). Since $Q = \epsilon \ll d\Lambda$, both K and $K+Q$ lie on the same side of the filling surface for all eligible choices of K. As a result, the directional integral of K is over the full range,

$$\begin{aligned} dF(\mathbf{n}_1, \mathbf{n}_2) = &\int \frac{d\mathbf{n}}{(2\pi)^{d-1}} F(\mathbf{n}_1, \mathbf{n}) F(\mathbf{n}, \mathbf{n}_2) \\ &\int_{d\Lambda} \frac{dk}{2\pi} \int_{-\infty}^{\infty} \frac{d\omega}{2\pi} G(\omega, k) G(\omega, k+\epsilon). \end{aligned} \tag{25}$$

Here $F(\mathbf{n}_1, \mathbf{n}_3)$ represents the appropriate choice of F that satisfies the momentum and spin conservation at each vertex. The integral over dk lies inside the thin shells to be integrated out. However, there are two such shells. One of the shells lies inside the filling surface while the other is outside the filling surface. For the outer shell corresponding to $k \in [\Lambda - d\Lambda, \Lambda] > 0$, the states belong to the 0-occupancy region, which means we can replace the Green function by

$$G(\omega, k) = \frac{1}{i\omega - v_L k}. \tag{26}$$

For the inner shell, corresponding to $k \in [-\Lambda, -\Lambda + d\Lambda] < 0$, the states belong to the single-occupancy region, which means we can replace the Green function by

$$G(\omega, k) = \frac{1/2}{i\omega - v_L k} + \frac{1/2}{i\omega - v_L k - U}. \tag{27}$$

The poles in the ω plane do not contribute if they lie on the same side of the real axis. The only surviving contribution from ZS is thus

$$dF(\mathbf{n}_1,\mathbf{n}_2) = 2\int \frac{d\mathbf{n}}{(2\pi)^{d-1}} F(\mathbf{n}_1,\mathbf{n})F(\mathbf{n},\mathbf{n}_2) \int_{-\Lambda}^{-\Lambda+d\Lambda} \frac{dk}{2\pi}\int_{-\infty}^{\infty}\frac{d\omega}{2\pi}\frac{1/2}{i\omega - v_L k}\cdot\frac{1/2}{i\omega - v_L k - U}. \tag{28}$$

The integral over ω and k gives

$$\int_{d\Lambda}\frac{dk}{2\pi}\int_{-\infty}^{\infty}\frac{d\omega}{2\pi}\frac{1/2}{i\omega - v_L k}\cdot\frac{1/2}{i\omega - v_L k - U} = \frac{d\Lambda}{8\pi U}. \tag{29}$$

As U is strongly relevant, that is, $U' = s^{-2}U$, this contribution goes to zero much faster than $d\Lambda/\Lambda$. Thus the ZS diagram does not contribute to the RG analysis.

Now consider the ZS' diagram. Due to the momentum transfer Q of order K_L at the left vertex, not only is the magnitude of the loop momentum restricted to lie within the shell being eliminated but also its angle is restricted to a range of order $d\Lambda/K_L$. This suppression in ZS' diagrams contributes to $d\Lambda^2/\Lambda K_L$. The β function thus vanishes as we take the limit $d\Lambda/\Lambda \to 0$. As we show in the Appendix, the contribution from the Wick-violating terms is not thermodynamically extensive. Hence, there is no correction in any order.

Finally, the same kinematic reasons used to establish that ZS' vanishes can be adopted to show that the BCS diagram also does not renormalize F at one loop. Hence, the coupling constants for the forward scattering do not flow in this order because $\beta(F) = 0$.

This vanishing of the β-function includes the ferromagnetic interaction of the form $-J\sum_{k,k'}(n_{k,\uparrow}-n_{k,\downarrow})(n_{k',\uparrow}-n_{k',\downarrow})$. Such terms have scaling dimensions identical to F or more generally the Landau parameters $f(\mathbf{p},\mathbf{p}')$. They are subdominant to the HK term which has a scaling dimension -2. The HK fixed point should include the family of all such Landau parameters as they are marginal contributions to all levels. The real space orderings such as spin orderings, on the other hand, are subservient to this fixed point since we only care about a thin shell of momentum around the filling surfaces.

B. 2 Filling surfaces

When there are 2 filling surfaces, there are at most 4 independent solutions to $\mathbf{P} = \mathbf{K}_1 + \mathbf{K}_2$ as shown in Fig.5. The combined equation $\mathbf{P} = \mathbf{K}_1 + \mathbf{K}_2$ and $\mathbf{P} = \mathbf{K}_3 + \mathbf{K}_4$ thus have $4 \times 4 = 16$ independent solutions. There are still explicitly 3 spin configurations for each momentum solution. Thus the total number of marginal forward scattering is $16 \times 3 = 48$. We will not enumerate them here since they remain non-contributing in the same way as we discussed in the case of a single-filling surface. The 1-loop correction contributes a term proportional to either $d\Lambda/U$ from the ZS diagrams or $d\Lambda/K_L$ for the ZS' and BCS diagrams. Once again, forward scatterings remain fixed under RG; that is, they do not flow under RG.

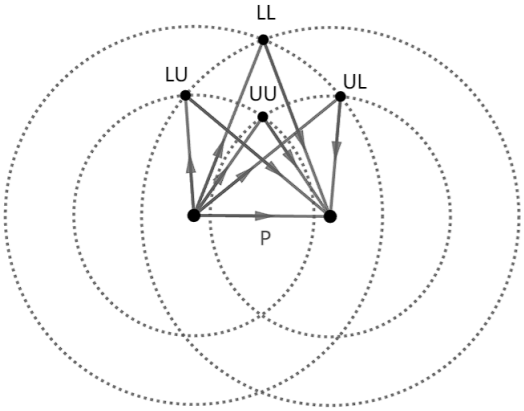

FIG. 5. The solutions to $\mathbf{P} = \mathbf{K}_1 + \mathbf{K}_2$. The L-surface and U-surface are plotted in dotted circles. The 4 solutions are marked by the surfaces where the 2 momentum that sum up to $\mathbf{P}$ are.

VI. SUPERCONDUCTING PAIRINGS AT 1-LOOP

The incoming and outgoing momenta each summing to zero $\mathbf{K}_1 = -\mathbf{K}_2, \mathbf{K}_3 = -\mathbf{K}_4$ constitute superconducting pairings. The 1-loop evolution of Vs has a non-vanishing contribution even for a Fermi liquid and hence we expect an analogous contribution at the HK fixed point should one exist. We will analyze the single and two filling surfaces separately.

A. 1 Filling surface

$\mathbf{K}_1$ and $\mathbf{K}_3$ can lie freely on the filling surface. For simplicity, we set all external legs to zero frequency and on the filling surface ($\omega = k = 0$). Including the spin-singlet and spin-triplet pairings, we have 2 choices,

$$V^1(\mathbf{n}_1,\mathbf{n}_3) = u(-\mathbf{K}_3\sigma, \mathbf{K}_3\sigma, -\mathbf{K}_1\sigma, \mathbf{K}_1\sigma), \tag{30}$$

$$V^2(\mathbf{n}_1,\mathbf{n}_3) = u(-\mathbf{K}_3\bar{\sigma}, \mathbf{K}_3\sigma, -\mathbf{K}_1\bar{\sigma}, \mathbf{K}_1\sigma). \tag{31}$$

These two spin configurations satisfy the antisymmetry for Fermions regardless of the angular structure of the pairing interaction. The incoming momenta are equal and opposite on the filling surface. The ZS and ZS' diagrams are suppressed by $d\Lambda^2/\Lambda K_L$ and hence do not contribute for the same reason that ZS' and BCS diagrams did not contribute to the flow of forward scatterings. The BCS diagram now has a contribution since the running momentum in the loop can now freely point in any direction, regardless of the value of K. We rewrite Eq.(21) as

$$dV^{1,2}(\mathbf{n}_1,\mathbf{n}_3) = -\frac{1}{2}\int\frac{d\mathbf{n}}{(2\pi)^{d-1}}V^{1,2}(\mathbf{n}_1,\mathbf{n})V^{1,2}(\mathbf{n},\mathbf{n}_3) \int_{d\Lambda}\frac{dk}{2\pi}\int_{-\infty}^{\infty}d\omega G(\omega,k)G(-\omega,k). \tag{32}$$

The integral over dk also lies inside the two thin shells to be integrated out. These two thin shells contribute differently.

For the outer shell, corresponding to $k \in [\Lambda - d\Lambda, \Lambda] > 0$, the second line of Eq.(32) yields a finite value $\frac{d\Lambda}{4\pi\Lambda v_L}$. For the inner shell, corresponding to $k \in [-\Lambda, -\Lambda + d\Lambda] < 0$, the integral region thus gives a value that is reduced by a factor of a quarter, $\frac{d\Lambda}{16\pi\Lambda v_L}$. In all, The renormalization group equation for $V^{1,2}$ is

$$\begin{aligned}\frac{dV(\mathbf{n}_1,\mathbf{n}_3)}{dt} &= -\frac{5}{32\pi v_L}\int \frac{d\mathbf{n}}{(2\pi)^{d-1}} V(\mathbf{n}_1,\mathbf{n})V(\mathbf{n},\mathbf{n}_3) \\ &\equiv -\frac{5}{32\pi v_L}(V*V)(\mathbf{n}_1,\mathbf{n}_3),\end{aligned} \tag{33}$$

where $dt = |d\Lambda|/\Lambda$ is the RG transform step size, and $*$ defines the generalized convolution in d-dimensions. This is the Cooper instability in the HK model. For the case of $d = 2$, we can simplify this by going to momentum eigenfunctions

$$V_l = \int_0^{2\pi} \frac{d\theta}{2\pi} e^{il\theta} V(\theta), \tag{34}$$

where $V(\theta) = V(\mathbf{n}_0, R_\theta \mathbf{n}_0)$ and R_θ is the rotation by degree θ. We can obtain the β function for each angular momentum l

$$\frac{dV_l}{dt} = -\frac{5}{32\pi v_L} V_l^2. \tag{35}$$

The flow tells us that the couplings V_l are marginally relevant if negative, and marginally irrelevant if positive. By integrating the flow, we obtain

$$V_l(t) = \frac{V_l(0)}{1 + 5tV_l(0)/32\pi v_L}, \tag{36}$$

which implies an instability at the energy scale $\Lambda_c = \Lambda_0 e^{32\pi v_L/5V_0}$. The energy scale in a thermal system is proportional to the temperature; thus we propose that the approximate transition temperature of this metallic state scales as Λ_c.

B. 2 Filling surfaces

The two-filling surfaces case remains to be analyzed. The electrons around different filling surfaces now have different contributions and are grouped into 3 different categories (intra-L, intra-U, and inter-LU)

$$V^1(\mathbf{n}_1,\mathbf{n}_3) = u(-\mathbf{K}_3^L\bar{\sigma}, \mathbf{K}_3^L\sigma, -\mathbf{K}_1^L\bar{\sigma}, \mathbf{K}_1^L\sigma), \tag{37}$$

$$V^2(\mathbf{n}_1,\mathbf{n}_3) = u(-\mathbf{K}_3^U\bar{\sigma}, \mathbf{K}_3^U\sigma, -\mathbf{K}_1^U\bar{\sigma}, \mathbf{K}_1^U\sigma), \tag{38}$$

$$V^3(\mathbf{n}_1,\mathbf{n}_3) = u(-\mathbf{K}_3^U\bar{\sigma}, \mathbf{K}_3^U\sigma, -\mathbf{K}_1^L\bar{\sigma}, \mathbf{K}_1^L\sigma), \tag{39}$$

for the spin-singlet configuration. Here the superscripts represent the surface around which the momenta are located. The spin-triplet processes have exactly the same RG structure and follow the same RG equations. We omit their definition and work with only the spin-singlet processes.

The RG flow of the BCS couplings still follows Eq.(32). The integral of the Green function around each filling surface follows the same process as Eq.(33). The renormalization group equations are

$$\frac{dV^1}{dt} = -\frac{5}{32\pi}\left(\frac{V^1 * V^1}{v_L} + \frac{V^{3\dagger} * V^3}{v_U}\right), \tag{40}$$

$$\frac{dV^2}{dt} = -\frac{5}{32\pi}\left(\frac{V^3 * V^{3\dagger}}{v_L} + \frac{V^2 * V^2}{v_U}\right), \tag{41}$$

$$\frac{dV^3}{dt} = -\frac{5}{32\pi}\left(\frac{V^1 * V^3}{v_L} + \frac{V^3 * V^2}{v_U}\right). \tag{42}$$

With the natural choice, $V^1 = V^2 = V^3 = V \in \mathbb{R}$, we simplify the β function to a single equation,

$$\frac{dV}{dt} = -\frac{5}{32\pi}\left(\frac{1}{v_L} + \frac{1}{v_U}\right) V * V. \tag{43}$$

For the case of $d = 2$, the instability for attractive V obtains at the energy scale

$$\Lambda_c = \Lambda_0 \exp\left(\frac{32\pi v_L v_U}{5(v_L + v_U)V_0}\right). \tag{44}$$

The energy scale in a thermal system is proportional to the temperature. This increase in the critical energy scale is consistent with the exactly calculated pair susceptibility[22], which diverges at a higher temperature for a small value of U compared with the Fermi liquid result. The comparison between different T_c was shown in Figure(6)

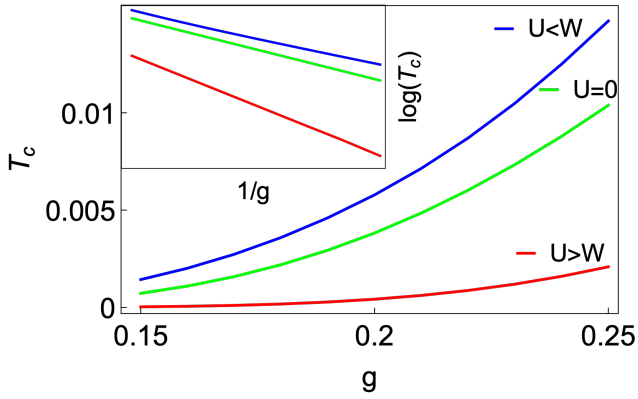

FIG. 6. The T_c (divergence of pair susceptibility) vs the superconducting pairing strength $g = -V$. The curves from top to bottom are: $U < W$ (2 filling surfaces), $U = 0$ (Fermi liquid), and $U > W$ (1 filling surface). The insert plot shows the linear dependence of $\log(T_c)$ on $1/g$ and the slope of each curve is $0.8 : 1 : 1.6$. These T_c exponents are consistent with the Λ_c estimate.

Due to the fact that RG analysis only deals with perturbative interactions around the fixed point at each step, the first-order transition into a superconductor at finite U[22] is absent.

VII. FINAL REMARKS

We have shown that the analogies with Fermi liquid theory noted in the introduction are borne out by a thorough RG analysis of the interactions that can contribute to the HK

model. For short-range repulsions, nothing flows away from HK, thereby establishing it as a stable fixed point depicted in Fig. (7). While it is surprising that a new quartic fixed point exists, it is ultimately not surprising given that the momentum structure of the HK model is identical to that of Fermi liquid theory. As a consequence, all of the interactions that flow into Fermi liquid theory also flow into this quartic fixed point. Once again as in Fermi liquid theory, superconductivity leads to flow away from the HK fixed point (see Fig.7). Since Hubbard interactions are also local in real space, they also cannot perturb away from the HK fixed point in the metallic state. This is crucial because there is much physics in the Hubbard model that is not present in the HK model. Local moment physics, antiferromagnetism, pseudogap physics, etc. are all consequences of Mottness, that is the movement of spectral weight from high to low energy upon the removal of single charges from the Mott state. Experimentally this is well documented in optical conductivity experiments[17].

Our focus on the simplest model for Zeroes of the Green function is based on the fact that they are essential for the movement of spectral weight at Mott scales. As such they are often used as a diagnosis[23, 24] of the pseudogap phase in the cuprates. The argument for zeroes being inextricably essential to Fermi arcs (either a nodal metal or a connected region of poles that does not extend to the zone boundary) is simple[24]. Consider the extreme case of a nodal metal in which a quasiparticle exists only at $(\pi/2, \pi/2)$. Consider traversing a path through $(\pi/2, \pi/2)$ and then returning along a path that does not cross this point. Then $ReG(p, \omega)$ must change sign for the momentum passing through the singularity at $(\pi/2, \pi/2)$. To end up with the correct sign for Re G, the return path must intersect a line across which $ReG(\omega = 0, p)$ changes sign. Since there are no infinities, except at $(\pi/2, \pi/2)$, the only option is for a zero line to exist. The zero line must emanate from the $(\pi, \pi/2)$ point and touch the edges of the Brillouin zone close to $(\pi, 0)$ and $(0, \pi)$. This argument is independent of the length of the region of poles (quasiparticles), that is if the nodal metal is extended to an actual arc that falls short of touching the BZ boundary. That we have found a solvable model for zeroes and established it as a fixed point illustrates that the physics of doped Mott insulators can be established independent of the Hubbard model. Indeed, the simplicity of the HK model belies its true robustness and generality.

While the similarity of the momentum structure of the theory with that of Fermi liquid theory plays a key role in the stability of the fixed point, the relation to Hubbard is ultimately driven by the Z_2 symmetry breaking of the interaction in Eq. (1). As long as the interaction is repulsive, breaking the Z_2 symmetry noted by Anderson and Haldane[20] leads to single occupancy. The phase diagram for the evolution of HK physics from a simple Fermi liquid is plotted as a function of the singly occupied region, Ω_1, as shown in Fig. (8). Fermi liquids live only in the region where Ω_1 vanishes. The transition line for superconductivity from a FL state is given by the green line. The entire region in the $\Omega_1 - g$ plane represents non-BCS superconductivity and is governed by the quartic HK fixed point delineated here. In addition to mediating non-Fermi liquid behavior, single occupancy in

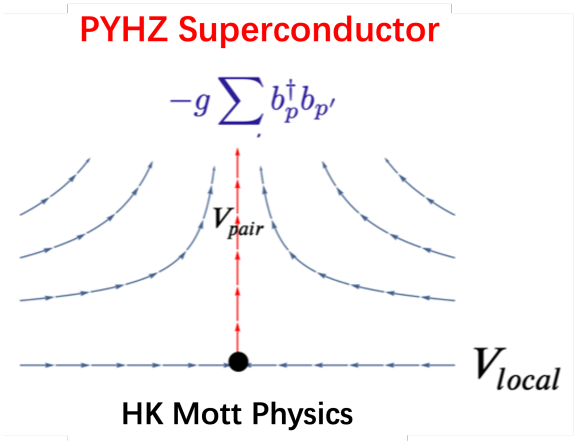

FIG. 7. Perturbative flow diagram for interactions in a doped HK Mott system. Short-range interactions regardless of their sign do nothing. Only pairing leads to flow to strong coupling and the ultimate destruction of the non-Fermi liquid HK metallic state and the onset of a superconducting state distinct from that of a BCS superconductor. The nature of the superconducting state cannot be established based on perturbative arguments but requires the PYH theory[13, 22].

real or momentum space leads to degeneracy. The degeneracy at half-filling could be lifted by considering a multi-orbital version of the HK model while preserving the key feature of Mott physics, namely the zeroes of the single-particle Green function[16].Away from half-filling, we show in Appendix C that an analogy of the Kohn-Luttinger[15] instability is present for the HK model appended with a general repulsive interaction. As such superconductivity also lifts the degeneracy, there is no $T = 0$ entropy problem in either the half-filled Mott insulator or the metallic state of the doped HK model, orbital or otherwise.

Essentially what the HK model does is separate the bifurcation of the spectral function into low and high energy branches per momentum state, the inherent physics of a Mott insulator, from ordering tendencies. Such ordering, antiferromagnetism or any other order associated with the pseudogap is governed by operators that have more than one momentum index and hence do not generate flow away from the stable metallic HK fixed point. Hence, what the HK model ultimately does is offer a way of treating Mott's original conception of the gapped half-filled band. Mottness sets the scale for the gap and ordering is secondary as borne out experimentally in all Mott systems ranging from the vanadates[25] to the cuprates[17, 26, 27].

Acknowledgements We thank the NSF DMR-2111379 for partial funding this work.

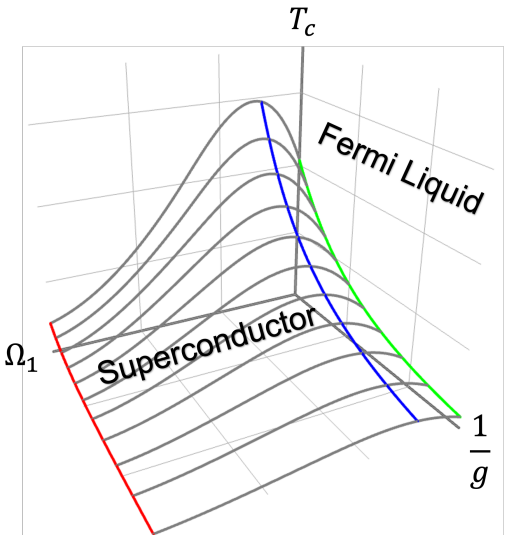

FIG. 8. The general phase diagram of the superconducting instability in the HK fixed point. As long as the Ω_1 region is non-zero, the system breaks the Fermi Liquid Z_2 symmetry and flows into HK.

APPENDIX

A. Detailed derivation of the Green function

Here we briefly review the exact partition and Green function of the HK model at any filling. We start with the HK Hamiltonian,

$$H_{HK} = \sum_k \left[\xi_k(n_{k\uparrow} + n_{k\downarrow}) + U n_{k\uparrow} n_{k\downarrow}\right], \tag{45}$$

where $\xi_k = \epsilon_k - \mu$. For each momentum sector, the HK Hamiltonian is built out of commuting parts. Thus, the partition function factorizes, and for each momentum sector we have

$$Z_k = 1 + 2e^{-\beta\xi_k} + e^{-\beta(2\xi_k+U)}. \tag{46}$$

The Heisenberg equations in imaginary time for Fermion $c_{k\sigma}$ annihilation and the number operator $n_{k\sigma} = c^\dagger_{k\sigma} c_{k\sigma}$ are

$$\dot{c}_{k\sigma} = [H, c_{k,\sigma}] = -(\xi_k + U n_{k\bar{\sigma}}) c_{k\sigma}, \tag{47}$$
$$\dot{n}_{k\sigma} = [H, n_{k,\sigma}] = 0. \tag{48}$$

Thus we have the time evolution of the fermi operator,

$$c_{k\sigma}(\tau) = e^{-(\xi_k + U n_{k\bar{\sigma}})\tau} c_{k\sigma}(0). \tag{49}$$

The average particle number is

$$\langle n_{k\sigma}\rangle = \frac{e^{-\beta\xi_k} + e^{-\beta(2\xi_k+U)}}{1 + 2e^{-\beta\xi_k} + e^{-\beta(2\xi_k+U)}}. \tag{50}$$

The imaginary time Green function is

$$\begin{aligned} G_{k\sigma}(\tau) &= -\langle c_{k\sigma}(\tau) c^\dagger_{k\sigma}(0)\rangle \\ &= -\mathrm{Tr}\left[e^{-\beta(H-F)} e^{-(\xi_k + U n_{k\bar{\sigma}})\tau} c_{k\sigma}(0) c^\dagger_{k\sigma}(0)\right] \\ &= -\mathrm{Tr}\left[e^{\beta F} e^{-(\xi_k + U n_{k\bar{\sigma}})\tau} e^{-\beta H}(1 - n_{k\sigma})\right] \\ &= -\frac{1}{Z_k}\left[e^{-\xi_k\tau} + e^{-\beta\xi_k} e^{-(\xi_k+U)\tau}\right]. \end{aligned} \tag{51}$$

Performing the Fourier transform with the anti-periodic boundary condition $G(\tau+\beta) = -G(\tau)$ leads to

$$\begin{aligned} G_{k\sigma}(i\omega_n) &= \int_0^\beta G_{k\sigma}(\tau) e^{i\omega_n\tau} \\ &= -\frac{1}{Z_k}\left[\frac{-e^{-\beta\xi_k} - 1}{i\omega_n - \xi_k} + e^{-\beta\xi_k}\frac{-e^{-\beta(\xi_k+U)} - 1}{i\omega_n - \xi_k - U}\right] \\ &= \frac{1 - \langle n_{k\bar{\sigma}}\rangle}{i\omega_n - \xi_k} + \frac{\langle n_{k\bar{\sigma}}\rangle}{i\omega_n - \xi_k - U}. \end{aligned} \tag{52}$$

This result is exact for any value of μ and U.

B. Weak coupling Expansion and Wick's Theorem

According to the Gell-Mann-Low formula, the $2n$-point function under interaction V is given by

$$\begin{aligned} &\langle T c^\dagger_{k_1}(\tau_1)\cdots c^\dagger_{k_n}(\tau_n) c_{k'_1}(\tau'_1)\cdots c_{k'_n}(\tau'_n)\rangle_I \\ &= \frac{\langle T \bar{c}_{k_1}(\tau_1)\cdots\bar{c}_{k_n}(\tau_n) c_{k'_1}(\tau'_1)\cdots c_{k'_n}(\tau'_n)\exp\left(-\int_0^\beta d\tau V[\bar{c}, c]\right)\rangle_{HK}}{\langle T\exp\left(-\int_0^\beta d\tau V[\bar{c}, c]\right)\rangle_{HK}}, \end{aligned} \tag{53}$$

where $\langle\rangle_I$ is the average using the full Hamiltonian $H_{HK} + H_I$ and $\langle\rangle_{HK}$ is the average under the HK Hamiltonian H_{HK} only.

Since the HK path integral is decomposed into a series of products in the momentum space, the creation and annihilation operators from different momentum sectors can be safely factored out. For example, suppose $k_1, k_2, \cdots, k_n$ are different from each other, and each corresponding annihilation and creation operator appears $l_1, l_2, \cdots, l_n$ times, then

$$\begin{aligned} &\left\langle T\prod_{j=1}^{l_1} c^\dagger_{k_1\sigma_1^j}(\tau_1^j)\cdots\prod_{j=1}^{l_n} c^\dagger_{k_n\sigma_n^j}(\tau_n^j)\prod_{j=1}^{l_1} c_{k_1\sigma_1^j}(\tau_1'^j)\cdots\prod_{j=1}^{l_n} c_{k_n\sigma_n^j}(\tau_n'^j)\right\rangle_{HK} \\ &= (-1)^P\left\langle T\prod_{j=1}^{l_1} c^\dagger_{k_1\sigma_1^j}(\tau_1^j)\prod_{j=1}^{l_1} c_{k_1\sigma_1^j}(\tau_1'^j)\right\rangle_{HK}\cdots\left\langle T\prod_{j=1}^{l_n} c^\dagger_{k_n\sigma_n^j}(\tau_n^j)\prod_{j=1}^{l_n} c_{k_n\sigma_n^j}(\tau_n'^j)\right\rangle_{HK}, \end{aligned} \tag{54}$$

where P is the times of permutation performed so as to separate the fermion operators.

The deviation from Wick's theorem could be observed on certain multi-point correlation functions(e.g. 4-point function) for which all the momenta of the fermion operators are identical. This contribution, however, is thermodynamically suppressed in our calculation. Thus we employ Feynman diagram rules and use the exact Green function to calculate the correlation functions.

C. Kohn-Luttinger Instability

Back in 1965, Kohn and Luttinger (KL)[28] pointed out that a Fermi liquid is never a zero-temperature state of matter as a result of an intrinsic tendency to form a superconductor. We illustrate that the same is true for the metallic state of HK. In principle, any system that has a Fermi surface will face BCS instability at low temperatures even if the initial coupling is repulsive. The KL statement stems from the observation that the screening around the Fermi surface contributes to a long-range oscillatory potential of the form $\cos(2k_F r)/r^3$, the Friedel oscillation[29]. The negative contribution gives rise to a superconducting instability in any system with a sharp Fermi surface.

Here we take advantage of the RG formalism and follow the derivation given by Shankar[19] in order to prove the same instability is entailed by the HK fixed point. For simplicity, we illustrate this in the case of only 1 lower-filling surface in 3d. Consider the ZS diagram as shown in Fig.4 which generates the BCS amplitude to one loop,

$$dV(\mathbf{n}_1,\mathbf{n}_3) = F(\pi)^2 \int \frac{dkd\mathbf{n}}{(2\pi)^d} \int_{-\infty}^{\infty} \frac{d\omega}{2\pi} G(\omega,k)G(\omega,k'), \tag{55}$$

where $F(\pi)$ is the backward scattering amplitude that enters both vertices and $k' = |\mathbf{K}'| - K_L$ refer to $\mathbf{K}' = \mathbf{K} + \mathbf{Q}$. The poles in the ω plane do not contribute if they lie on the same side of the real axis. When both $\mathbf{K}$ and $\mathbf{K}'$ live outside the filling surface, $k, k' > 0$, their Green function takes the form of Eq.(26) and gives no contribution upon integrating along ω. For both $\mathbf{K}$ and $\mathbf{K}'$ living inside the filling surface, $k, k' < 0$. Their Green function takes the form of Eq.(27), and gives a contribution proportional to

$$-\frac{1}{4}F(\pi)^2 \int \frac{dkd\mathbf{n}}{(2\pi)^d} \theta(-k)\theta(-k') \left(\frac{1}{E(\mathbf{K}') - E(\mathbf{K}) + U} + \frac{1}{E(\mathbf{K}') - E(\mathbf{K}) - U} \right). \tag{56}$$

This contribution becomes strongly suppressed by $1/U$ and thus does not modify the RG. The only non-vanishing contribution comes from $\mathbf{K}$ and $\mathbf{K}'$ lie on different sides of the filling surface, that is, $k > 0, k' < 0$ or $k < 0, k' > 0$. The amplitude is thus

$$-\frac{1}{2}F(\pi)^2 \int \frac{dkd\mathbf{n}}{(2\pi)^d} \left(\frac{\theta(-k)\theta(k')}{E(\mathbf{K}') - E(\mathbf{K})} + \frac{\theta(k)\theta(-k')}{E(\mathbf{K}) - E(\mathbf{K}')} \right). \tag{57}$$

This is exactly half the contribution of the Kohn-Luttinger amplitude in Fermi liquid[19] theory. Thus, integrating out the momenta and frequency as is standard yields the RG equation

$$\frac{dV_l}{dt} = -\frac{5}{32\pi v_L} V_l^2 - \frac{V(\pi)^2 \lambda^{7/4}}{2l^{15/2}(\lambda^{7/4} + l^{-7/2}) v_L}, \tag{58}$$

where $\lambda = \Lambda/K_L$. The second term vanishes as $(\Lambda/K_L)^{7/4}$ as $\Lambda \to 0$. However, $V_l \propto e^{-l}$ as $l \to \infty$. It is clear that as soon as the flow begins, the exponentially small initial coupling $V_l(0)$ will very quickly be driven to negative values by the second term, and the superconducting instability driven by the first term emerges. Thus, just as in Fermi liquid, the HK fixed point is not a zero temperature fixed point either. As the temperature lowers, the ground state is always superconducting without degeneracy[22].

D. Magnetic instability

The singly occupied region of the HK model at finite U in the HK model leads to a singly occupied region which introduces spin degeneracy for each momentum sector. This ground state degeneracy is extensive with the system size and thus considered to be unphysical although a singly occupied region generally exists in Mott systems with the traditional Hubbard model. The solution to the degeneracy in the HK fixed point is ordering such as superconductivity, ferromagnetism, or a spin-density wave. The superconducting instability has been discussed in the main body and we provide here an analysis of a possible magnetic ordering of the HK model.

With an external magnetic field B, the partition function now reads,

$$Z(B) = \sum_k \left(1 + e^{-\beta(\xi_k - \mu B)} + e^{-\beta(\xi_k + \mu B)} + e^{-\beta(2\xi_k + U)} \right). \tag{59}$$

The magnetic susceptibility is achieved by a double derivative of the partition function,

$$\begin{aligned} \chi &= -\frac{1}{\beta Z(B)} \frac{\partial^2 Z}{\partial B^2}\bigg|_{B=0} \\ &= \frac{\mu^2 \beta}{Z(B)} \sum_k \left(e^{-\beta(\xi_k - \mu B)} + e^{-\beta(\xi_k + \mu B)} \right)\bigg|_{B=0} \\ &= \mu^2 \Omega_1 \beta, \end{aligned} \tag{60}$$

where Ω_1 is the extent of the singly occupied region. The susceptibility diverges as temperature goes to zero, signaling a ferromagnetic phase transition at $T = 0$. As pointed out in the previous section, at low temperatures the interacting HK system always has a superconducting instability which lifts the degeneracy. This ferromagnetic instability is covered up by the superconducting phase.

[1] Y. Hatsugai and M. Kohmoto, Exactly solvable model of correlated lattice electrons in any dimensions, Journal of the Physical Society of Japan **61**, 2056 (1992), https://doi.org/10.1143/JPSJ.61.2056.

[2] Y. Li, V. Mishra, Y. Zhou, and F.-C. Zhang, Two-stage superconductivity in the hatsugaikohomoto-bcs model, New Journal of Physics **24**, 103019 (2022).

[3] Y. Zhong, Solvable periodic anderson model with infinite-range hatsugai-kohmoto interaction: Ground-states and beyond, Phys. Rev. B **106**, 155119 (2022).

[4] K. Yang, Exactly solvable model of fermi arcs and pseudogap, Phys. Rev. B **103**, 024529 (2021).

[5] C. Setty, Superconductivity from luttinger surfaces: Emergent sachdev-ye-kitaev physics with infinite-body interactions, Phys. Rev. B **103**, 014501 (2021).

[6] H.-S. Zhu, Z. Li, Q. Han, and Z. D. Wang, Topological s-wave superconductors driven by electron correlation, Phys. Rev. B **103**, 024514 (2021).

[7] V. Leeb and J. Knolle, Quantum oscillations in a doped Mott insulator beyond Onsager's relation, arXiv e-prints , arXiv:2301.08685 (2023), arXiv:2301.08685 [cond-mat.str-el].

[8] H.-S. Zhu and Q. Han, Effects of electron correlation on superconductivity in the hatsugai kohmoto model*, Chinese Physics B **30**, 107401 (2021).

[9] C. Setty, Dilute magnetic moments in an exactly solvable interacting host (2021), arXiv:2105.15205 [cond-mat.str-el].

[10] Y.-C. Tzeng, P.-Y. Chang, and M.-F. Yang, Interaction-induced metal to topological insulator transition (2023), arXiv:2302.02771 [cond-mat.str-el].

[11] Y. Zhong, Notes on quantum oscillation for hatsugai-kohmoto model (2023), arXiv:2301.09377 [cond-mat.str-el].

[12] M. Zhao, W.-W. Yang, H.-G. Luo, and Y. Zhong, Friedel oscillation in non-Fermi liquid: Lesson from exactly solvable Hatsugai-Kohmoto model, arXiv e-prints , arXiv:2303.00926 (2023), arXiv:2303.00926 [cond-mat.str-el].

[13] P. W. Phillips, L. Yeo, and E. W. Huang, Exact theory for superconductivity in a doped mott insulator, Nature Physics **16**, 1175 (2020).

[14] E. W. Huang, G. L. Nave, and P. W. Phillips, Discrete symmetry breaking defines the mott quartic fixed point, Nature Physics **18**, 511 (2022).

[15] W. Kohn and J. M. Luttinger, New mechanism for superconductivity, Phys. Rev. Lett. **15**, 524 (1965).

[16] D. Manning-Coe and B. Bradlyn, Ground state stability, symmetry, and degeneracy in Mott insulators with long range interactions, arXiv e-prints , arXiv:2306.00221 (2023), arXiv:2306.00221 [cond-mat.str-el].

[17] S. Uchida, T. Ido, H. Takagi, T. Arima, Y. Tokura, and S. Tajima, Optical spectra of $\mathrm{la_{2-x}sr_xcuo_4}$: Effect of carrier doping on the electronic structure of the $\mathrm{cuo_2}$ plane, Phys. Rev. B **43**, 7942 (1991).

[18] J. Polchinski, Effective field theory and the fermi surface, arXiv:hep-th/9210046v2 (1992).

[19] R. Shankar, Renormalization-group approach to interacting fermions, Rev. Mod. Phys. **66**, 129 (1994).

[20] P. W. Anderson and F. D. M. Haldane, The symmetries of fermion fluids at low dimensions, Journal of Statistical Physics **103**, 425 (2001).

[21] S. Weinberg, Volume ii, in *The Quantum Theory of Fields*, Vol. 2 (Cambridge University Press, 1996) pp. xvii–xix.

[22] J. Zhao, L. Yeo, E. W. Huang, and P. W. Phillips, Thermodynamics of an exactly solvable model for superconductivity in a doped mott insulator, Physical Review B **105**, 184509 (2022).

[23] T. D. Stanescu and G. Kotliar, Fermi arcs and hidden zeros of the green function in the pseudogap state, Phys. Rev. B **74**, 125110 (2006).

[24] T. D. Stanescu, P. Phillips, and T.-P. Choy, Theory of the luttinger surface in doped mott insulators, Phys. Rev. B **75**, 104503 (2007).

[25] M. M. Qazilbash, A. A. Schafgans, K. S. Burch, S. J. Yun, B. G. Chae, B. J. Kim, H. T. Kim, and D. N. Basov, Electrodynamics of the vanadium oxides $\mathrm{Vo_2}$ and $\mathrm{v_2o_3}$, Phys. Rev. B **77**, 115121 (2008).

[26] S. L. Cooper, G. A. Thomas, J. Orenstein, D. H. Rapkine, A. J. Millis, S.-W. Cheong, A. S. Cooper, and Z. Fisk, Growth of the optical conductivity in the cu-o planes, Phys. Rev. B **41**, 11605 (1990).

[27] C. T. Chen, F. Sette, Y. Ma, M. S. Hybertsen, E. B. Stechel, W. M. C. Foulkes, M. Schulter, S.-W. Cheong, A. S. Cooper, L. W. Rupp, B. Batlogg, Y. L. Soo, Z. H. Ming, A. Krol, and Y. H. Kao, Electronic states in $\mathrm{la_{2-x}sr_xcuo_{4+\delta}}$ probed by soft-x-ray absorption, Phys. Rev. Lett. **66**, 104 (1991).

[28] W. Kohn and J. Luttinger, New mechanism for superconductivity, Physical Review Letters **15**, 524 (1965).

[29] J. Friedel, Electronic structure of primary solid solutions in metals, Advances in Physics **3**, 446 (1954).